Plate arrays as a perfectly-transmitting negative refraction metamaterial

Richard Porter

School of Mathematics, University of Bristol, Bristol, BS8 1TW, UK

Abstract

A closely-spaced periodic array of identical thin rigid plates illuminated by incident waves is shown to act as a negative refraction metamaterial. The close-spacing assumption is used as a basis for an approximation in which the region occupied by the plate array acts as an effective medium. Effective matching conditions on the plate array boundary are also derived. The approximation allows explicit expressions to be derived to wave scattering problems involving titled plate arrays. This approximation is tested for its accuracy against an exact treatment of the problem based on Bloch-Floquet theory.

Both the exact and effective medium theory predict perfect wave transmission at *all* wave frequencies through the array when the tilt angle of plates in the array is the reverse of the incident wave direction: the array acts as an all-frequency perfectly-transmitting negative-refraction medium. For certain frequencies the array is also shown to act as an all-angle perfectly-transmitting negative-refraction material.

Keywords: Staggered plates; periodic array; homogenization; metamaterial; negative refraction.

1. Introduction

In this paper we consider the two-dimensional problem of the scattering of waves by a staggered infinite periodic array of thin parallel plates. The problem has a long history in acoustics with application to blade rows in turbomachinery. More recent papers in this application area often relate to circular duct geometries and include effects such as swirling flow in addition to basic mean flow; for example [1]. In earlier papers the simpler two-dimensional linear blade row was considered by [2], [3] and [4]. These three papers all consider periodic arrays of thin plates with stagger in the presence of mean flow (equations for the pressure field include a Mach number, M). The work of [3] and [4] employ the Wiener-Hopf method to derive solutions, extending earlier work of [5], [6] and [7] for arrays without stagger. They sought to improve upon the simple approximate method of [2] who matched solutions outside the array with a continuum model for the field inside the array based on infinitesimal separation between adjacent blades.

Email address: richard.porter@bristol.ac.uk (Richard Porter)

[2] highlighted that zeros of transmission at frequencies dependent on M could be found at incident angles opposed to the inclination of elements in array. In the three papers cited above involving stagger much of the focus of results concerns the influence of mean flow as this is pertinent to the application area. However, [2] also point out that without mean flow the transmitted and reflected wave amplitudes are symmetric with respect of the incident wave heading, regardless of stagger. This is certainly not an intuitive result. In this paper we confirm and extend this result with a different application area in mind.

The last 20 years has seen a vast expansion of interest in the science of so-called metamaterials. These are manufactured materials having properties not usually found in nature. A metamaterial typically possesses a microstructure whose effect upon the macroscopic field variables allows it to exhibit complex and counter-intuitive phenomena. The design and realisation of metamaterials have provided researchers with a range of new problems that can be considered. One of the key demands of metamaterials in wave engineering problems such as invisibility cloaking or perfect lensing is the ability to be able to redirect the path of waves without reflection and with a negative refractive index. For example, see [8], [9], [10] and [11] for examples related closely to the current work.

In this paper we bring together the ideas of closely-spaced plate arrays and metamaterials to illustrate two principal effects: (i) all-frequency perfectly-transmitting negative refraction based wave shifting; and (ii) all-angle perfectly-transmitting negative refraction wave shifting. We shall also illustrate trapping of waves by long finite-width staggered plate arrays.

Two approaches are taken to the solving the staggered plate array problem. After defining the problem in §2 we focus in §3 on formulating an approximation to the solution based on a close-spacing assumption. This is, in essence, the approach adopted by [2]. The effect of the microstructure is captured by reducing (through a formal asymptotic procedure) the wave equation to allow wave motion only in directions aligned with plates in the array. This process might be referred to as homogenisation/continuum modelling or effective field theory depending on the context. With the addition of effective boundary conditions between the plate array and the exterior domain we derive explicit solutions to a variety of problems illustrating various interesting wave effects indicated in the paragraph above as well as considering edge waves trapped within the plate array and their excitation by point sources in the neighbourhood of the plate array.

To confirm the validity of the approximation of §3, the problem of plane wave scattering, without approximation, by an infinite periodic array of thin staggered plates is considered in §4. Usual arguments, based on periodicity, are adopted to reduce the boundary-value problem to one that lies within a fundamental periodic strip of the domain and the application of Fourier transforms lead to integral equations which can be solved accurately and efficiently using well-established approximation methods. An analysis of the structure of this solution shows that all of the key symmetry and transparency relations present in the approximation are shared by this exact treatment of the problem. This approach appears to be much simpler than the ones used by [3] and [4].

Results are produced throughout the paper to demonstrate various aspects of the theory and the paper is concluded in §5.

2. Description of the problem

A periodic array is comprised of thin plates each of length $2L$, separated from their neighbours by a perpendicular distance d, with centres lying along $y = 0$ and tilted at an angle δ to the positive y-axis (see Fig. 1). The array occupies the strip $-b < y < b$, $-\infty < x < \infty$ such that $b = L\cos\delta$ and along the edges $y = \pm b$ the edges of adjacent plates are separated by a distance $l = d/\cos\delta$. The overlap (or stagger) between two adjacent plates in the array is $a = d\tan\delta$.

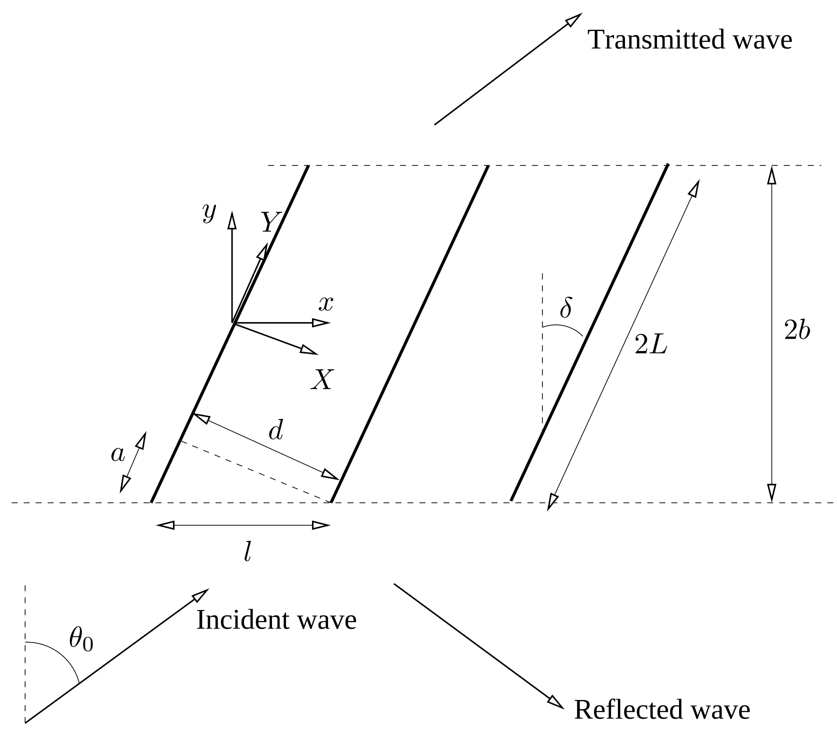

Figure 1: Definition sketch showing three thin plates within the periodic array.

The periodic array of plates is embedded in an infinite two-dimensional domain occupied by a homogeneous medium which supports wave propagation with phase speed c. Assuming time-harmonic motion of angular frequency ω the function $\phi(x, y)$ describing the field within the medium satisfies the two-dimensional wave equation

$$\left(\frac{\partial^2}{\partial x^2} + \frac{\partial^2}{\partial y^2} + k^2\right)\phi = 0 \tag{2.1}$$

where $k = \omega/c$ is the wavenumber. On both sides of each plate within the array ϕ satisfies a homogeneous Neumann boundary condition. Thus the problem can be interpreted in a number of different physical settings including low-Mach number linearised acoustics, linearised surface gravity waves on a fluid of constant depth and TM-polarised waves in electromagnetics.

An incident plane wave making an angle θ_0 with respect to the positive y-axis arrives from infinity in $y < -b$. It is described by the function

$$\phi_{inc}(x, y) = \mathrm{e}^{\mathrm{i}\alpha_0 x}\mathrm{e}^{\mathrm{i}\beta_0 y} \tag{2.2}$$

where $\alpha_0 = k\sin\theta_0$, $\beta_0 = k\cos\theta_0$ are wavenumber components in the x- and y-directions.

Far away from the array of plates, ϕ is assumed to satisfy

$$\phi(x, y) \sim \begin{cases} \phi_{inc}(x, y) + R\mathrm{e}^{\mathrm{i}\alpha_0 x}\mathrm{e}^{-\mathrm{i}\beta_0 y}, & \text{as } y \to -\infty \\ T\mathrm{e}^{\mathrm{i}\alpha_0 x}\mathrm{e}^{\mathrm{i}\beta_0 y}, & \text{as } y \to \infty \end{cases} \tag{2.3}$$

where R and T are the reflection and transmission coefficients and are the principal unknowns in the problem. The form of (2.3) holds provided kd is sufficiently small (otherwise higher-order diffraction modes are cut on) and we assume this to be the case here.

We also employ coordinates (X, Y) perpendicular and parallel (respectively) to the plates, related to (x, y) by

$$\begin{pmatrix} x \\ y \end{pmatrix} = \begin{pmatrix} \cos\delta & \sin\delta \\ -\sin\delta & \cos\delta \end{pmatrix}\begin{pmatrix} X \\ Y \end{pmatrix}. \tag{2.4}$$

Under this transformation (2.1) is replaced by

$$\left(\frac{\partial^2}{\partial X^2} + \frac{\partial^2}{\partial Y^2} + k^2\right)\psi = 0 \tag{2.5}$$

for $\psi(X, Y) = \phi(x, y)$ with boundary conditions on the plates are expressed as

$$\psi_X(X_n^{\pm}, Y) = 0, \qquad \text{for } -L < Y - X_n\tan\delta < L,\ n \in \mathbb{Z} \tag{2.6}$$

where $X_n = nd$.

3. Approximation for closely-spaced plates

An approximation is developed under the assumption that the spacing between the plates is small in relation to the plate length: $\epsilon = d/L \ll 1$. It is also assumed that $kL = O(1)$ which implies that $kd = O(\epsilon) \ll 1$. This implies the wavelength is much larger than the perpendicular distance between adjacent plates.

We start by considering the solution in $|y| < b$ in the domain occupied by the plate array. Every point in this domain can be written as $X = X_n + dX'$ and $Y = X_n \tan\delta + LY'$ where $X' \in (0,1)$, $-1 + \epsilon \tan\delta < Y' < 1$ and $-\infty < n < \infty$ and the corresponding solution is referenced as $\psi(X,Y) \equiv \psi_n(X',Y')$. Under this transformation, $\psi_n(X',Y')$ satisfies, from (2.5),

$$\frac{1}{\epsilon^2}\frac{\partial^2 \psi_n}{\partial X'^2} + \left(\frac{\partial^2}{\partial Y'^2} + k^2L^2\right)\psi_n = 0 \tag{3.1}$$

for $0 < X' < 1$ in which $\partial_{X'}\psi_n = 0$ on $X' = 0, 1$ from (2.6). The local solution is expanded powers of ϵ^2 as

$$\psi_n(X',Y') \approx \psi_n^{(0)}(X',Y') + \epsilon^2\psi_n^{(1)}(X',Y') + \ldots \tag{3.2}$$

where $\partial_{X'}\psi_n^{(m)} = 0$ on $X' = 0, 1$ for each m. At leading order $\partial_{X'X'}\psi_n^{(0)} = 0$ for $0 < X' < 1$ and along with the boundary conditions this gives us $\psi_n^{(0)} \equiv \psi_n^{(0)}(Y')$.

At next order (3.1) reads

$$\frac{\partial^2 \psi_n^{(1)}}{\partial X'^2} + \left(\frac{\partial^2}{\partial Y'^2} + k^2L^2\right)\psi_n^{(0)} = 0 \tag{3.3}$$

for $-1 + \epsilon\tan\delta < Y' < 1$, $0 < X' < 1$. Integrating (3.3) over $0 < X' < 1$ and using the boundary conditions at $X' = 0, 1$ results in

$$\left(\frac{\partial^2}{\partial Y'^2} + k^2L^2\right)\psi_n^{(0)} = 0 \tag{3.4}$$

over $|Y'| < 1$ (to leading order in ϵ) and so it follows that

$$\psi_n^{(0)}(Y') = C_n \mathrm{e}^{\mathrm{i}kLY'} + D_n \mathrm{e}^{-\mathrm{i}kLY'} \tag{3.5}$$

for arbitrary coefficients C_n and D_n. The solution (3.5) is as we expect on physical grounds: at leading order the waves are confined to propagate along in each narrow channel and amplitudes in different channels are independent.

3.1. *Plane wave scattering*

The values of C_n and D_n in (3.5) are determined by matching the solution in each channel to the solution in the regions exterior to the plate array and we consider this now. Since the geometry is periodic in x with period l, general solutions in $|y| > b$ can be determined using Bloch-Floquet theory which requires $\phi(x + l, y) = \mathrm{e}^{\mathrm{i}\alpha_0 l}\phi(x,y)$ and there is only a change in phase relating to the incident wave in the solution from one period to the next (this is revisited in §4). Thus, the general solution in $y < -b$ can be written

$$\phi(x, y) = \mathrm{e}^{\mathrm{i}\alpha_0 x}\left(\mathrm{e}^{\mathrm{i}\beta_0 y} + R\mathrm{e}^{-\mathrm{i}\beta_0 y} + \sum_{\substack{n=-\infty \\ \neq 0}}^{\infty} a_n \mathrm{e}^{\gamma_n y}\mathrm{e}^{2\pi n\mathrm{i}x/l}\right) \tag{3.6}$$

where a_n are undetermined coefficients and $\gamma_n = \sqrt{(\alpha_0 + 2n\pi/l)^2 - k^2}$. A similar expansion holds for $y > b$. Thus, terms contained in the infinite sum contribute to oscillations on the scale of the channel width, $d = l\cos\delta$, a scale not captured by approximation developed above. The first consequence of this is that the leading-order solution in $y < -b$ is reduced from (3.6) to

$$\phi(x, y) \approx \mathrm{e}^{\mathrm{i}\alpha_0 x}(\mathrm{e}^{\mathrm{i}\beta_0 y} + R\mathrm{e}^{-\mathrm{i}\beta_0 y}), \tag{3.7}$$

coinciding everywhere with the far-field representation, (2.3). Similarly for $y > b$ we approximate the solution by

$$\phi(x, y) \approx T\mathrm{e}^{\mathrm{i}\alpha_0 x}\mathrm{e}^{\mathrm{i}\beta_0 y}. \tag{3.8}$$

A second consequence is that the coefficients C_n and D_n introduced in (3.5) vary spatially with n, to leading order, over the lengthscale L and this justifies expressing the coefficients $C_n \equiv C(X_n)$ and $D_n \equiv D(X_n)$ as discrete evaluations of continuous functions. Under this assumption we can approximate the solution in the array (3.5) as

$$\psi(X, Y) = \psi_n(X', Y') \approx C(X)\mathrm{e}^{\mathrm{i}kY} + D(X)\mathrm{e}^{-\mathrm{i}kY}. \tag{3.9}$$

Transforming this solution back into original (x, y) variables through the use of (2.4) gives

$$\phi(x, y) \approx C(x\cos\delta - y\sin\delta)\mathrm{e}^{\mathrm{i}k(x\sin\delta + y\cos\delta)} + D(x\cos\delta - y\sin\delta)\mathrm{e}^{-\mathrm{i}k(x\sin\delta + y\cos\delta)} \tag{3.10}$$

within $|y| < b$. Matching the field variable, ϕ, across $y = \pm b$ over $-\infty < x < \infty$ in (3.7), (3.8) with (3.10) allows us to infer that the functions introduced in (3.9) must take the form

$$C(t) = C'\mathrm{e}^{\mathrm{i}(\alpha_0 - k\sin\delta)t/\cos\delta}, \qquad D(t) = D'\mathrm{e}^{\mathrm{i}(\alpha_0 - k\sin\delta)t/\cos\delta} \tag{3.11}$$

where $C', D' \in \mathbb{C}$ are constants. Using the definitions (3.11) in (3.10) reduces that equation to

$$\phi(x, y) \approx \left(C'\mathrm{e}^{\mathrm{i}ky/\cos\delta} + D'\mathrm{e}^{-\mathrm{i}ky/\cos\delta}\right)\mathrm{e}^{\mathrm{i}\alpha_0(x - y\tan\delta)}. \tag{3.12}$$

Additionally, matching the field variable ϕ across $y = -b$ and $y = b$ gives, respectively,

$$\mathrm{e}^{-\mathrm{i}\beta_0 b} + R\mathrm{e}^{\mathrm{i}\beta_0 b} = (C'\mathrm{e}^{-\mathrm{i}kL} + D'\mathrm{e}^{\mathrm{i}kL})\mathrm{e}^{\mathrm{i}\alpha_0 L\sin\delta} \tag{3.13}$$

and

$$Te^{i\beta_0 b} = (C'e^{ikL} + D'e^{-ikL})e^{-i\alpha_0 L \sin\delta}. \tag{3.14}$$

Fluxes must also be matched across boundaries between neighbouring domains. Equating flux within two adjacent plates, $d\psi_Y$, at $Y = \pm L$ to the flux, $l\phi_y$, across the boundaries $y = \pm b$ between the edges of those plates into the exterior domain through small connecting right-angled triangles (see Fig. 1) with sides of length a, d and l gives

$$\beta_0(e^{-i\beta_0 b} - Re^{i\beta_0 b}) = k\cos\delta(C'e^{-ikL} - D'e^{ikL})e^{i\alpha_0 L\sin\delta} \tag{3.15}$$

and

$$\beta_0 Te^{i\beta_0 b} = k\cos\delta(C'e^{ikL} - D'e^{-ikL})e^{-i\alpha_0 L\sin\delta}. \tag{3.16}$$

It is now simply a matter of eliminating between (3.13), (3.14), (3.15) and (3.16), a process which results in the following closed-form expressions for the reflection and transmission coefficients

$$R = \frac{(\cos^2\theta_0 - \cos^2\delta)\sin(2kL)e^{-2ikL\cos\theta_0\cos\delta}}{(\cos^2\theta_0 + \cos^2\delta)\sin(2kL) + 2i\cos(2kL)\cos\theta_0\cos\delta} \tag{3.17}$$

and

$$T = \frac{2i\cos\theta_0\cos\delta e^{-2ikL\cos(\theta_0-\delta)}}{(\cos^2\theta_0 + \cos^2\delta)\sin(2kL) + 2i\cos(2kL)\cos\theta_0\cos\delta}, \tag{3.18}$$

noting that $b = L\cos\delta$.

Several things are worthy of note here. First, the conservation of energy relation, $|R|^2 + |T|^2 = 1$, is easily verified from the expressions above. Next, various properties emerge from the relations (3.17), (3.18). Writing $R \equiv R(\theta_0, \delta, kL)$, $T \equiv T(\theta_0, \delta, kL)$ helps list those properties below.

(i) Symmetry, meaning

$$R(\theta_0, \delta, kL) = R(-\theta_0, \delta, kL), \qquad \text{and} \qquad R(\theta_0, \delta, kL) = R(\theta_0, -\delta, kL) \tag{3.19}$$

with the same relations applying to $|T|$.

(ii) Transparency, meaning that: (a)

$$R(\theta_0, \pm\theta_0, kL) = 0, \qquad \begin{cases} T(\theta_0, \theta_0, kL) = 1, \\ |T(\theta_0, -\theta_0, kL)| = 1; \end{cases} \tag{3.20}$$

and (b)

$$R(\theta_0, \delta, n\pi/2) = 0, \tag{3.21}$$

with $|T| = 1$ at $kL = n\pi/2$.

(iii) Reciprocity in angles, meaning

$$R(\theta_0, \delta, kL) = -R(\delta, \theta_0, kL), \qquad T(\theta_0, \delta, kL) = T(\delta, \theta_0, kL). \tag{3.22}$$

(iv) Wavenumber periodicity, meaning

$$|R(\theta_0, \theta_0, kL + n\pi/2)| = |R(\theta_0, \theta_0, kL)| \tag{3.23}$$

and

$$|R(\theta_0, \theta_0, \pi/2 - kL)| = |R(\theta_0, \theta_0, kL)| \tag{3.24}$$

with the same relations applying to $|T|$.

Amongst these results, most remarkable is the result (ii)(a) which states that total transmission occurs for all wavenumbers when $\theta_0 = -\delta$ and the angle of plates in the array is the reverse of the incident wave direction. An illustration of this result is given in Fig. 2 which shows the instantaneous wave field for a wave propagating at $\theta_0 = 45^\circ$ across an array of dimensionless width 2 tilted at $\delta = -45^\circ$. In the left-hand and right-hand panels, $kb = 1$ and $kb = 2$. Incoming waves are perfectly impedance matched at the boundary of the array and wave fronts are transmitted through the plate array in the reverse orientation before continuing in their original direction as they emerge at the far boundary of the array. Later figures in the paper help with this interpretation.

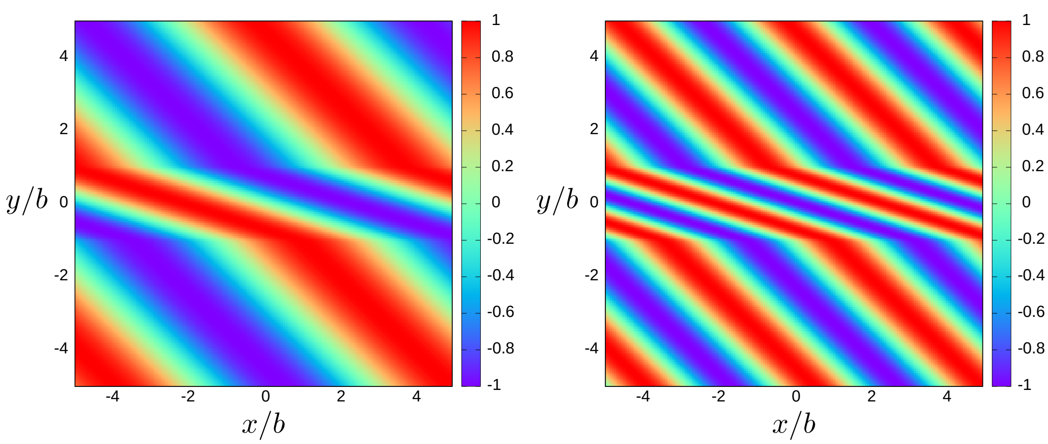

Figure 2: The instantaneous wave field for incident waves propagating at $\theta_0 = 45^\circ$ into an array of plates tilted at $\delta = -45^\circ$ for $kb = 1$ (left) and $kb = 2$ (right).

Fig. 3 shows the modulus of the reflection coefficient as a function of incident wave angles $\theta_0 \in [0^\circ, 90^\circ)$ for different array inclinations, δ, each for a fixed value of $kb = 2$. The results are symmetric in θ_0 (property (i) above) and we observe the vanishing of R when $\theta_0 = \delta$ (which must occur on physical grounds) and that $|R| \to 1$ as θ_0 approaches the grazing angle.

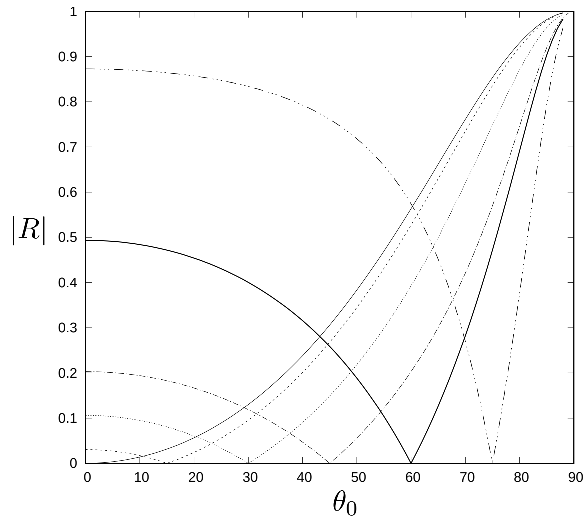

Figure 3: The variation of $|R|$ with θ_0 for $\delta = 0°, 15°, 30°, 45°, 60°, 75°$ when $kb = 2$.

3.2. Gaussian wavepacket

In Fig. 4 we provide an alternative illustration of the same features described in Fig. 2 by showing the evolution of a dispersive Gaussian wavepacket defined at $t = 0$ in the left-hand plot and evolving to the surface shown in the right-hand plot at $t = 6$s later. The wave field in Fig. 4 is defined to be the real part of

$$\frac{b}{\sqrt{4\sigma}} \int_{-\infty}^{\infty} \phi(x, y; k) \mathrm{e}^{-(kb-k_0 b)^2/(4\sigma)} \, \mathrm{e}^{-\mathrm{i}\omega t} \, dk \tag{3.25}$$

where the linear water wave dispersion relation $\omega = \sqrt{gk \tanh kh}$ has been used with $g = 9.81\text{ms}^{-2}$ and h the water depth. Here, $\phi(x, y; k)$ is the solution of §3.1, the dependence upon the wavenumber k having been made explicit. For the computation of Fig. 4 we have taken $k_0 b = \pi$, $h = 0.1$m, $g = 9.81\text{ms}^{-2}$, $b = 0.1$m, $\sigma = 0.2$ and all frequency components are propagating at $\theta_0 = 45°$. The integral in (3.25) is approximated by the rectangle rule and truncation of limits. Fig. 4 reinforces the perfect transmission of all frequency components of dispersive surface waves on water through a plate array tilted against the incident wave direction.

We have established that the plate array acts as a perfectly-transmitting negative refraction medium and the finite width of the array provides us with a 'metamaterial wave shifter' of the type described by [11]. An example of the potential application of such a device is shown in the sketch in Fig. 5 in which two parallel waveguides, offset laterally and connected by a junction, contains a closely-spaced array of plates oriented at the reverse angle to the waveguide walls. Ignoring any local effects caused in practice by the finite separation of the plates in the array, plane waves of all frequencies will propagate without reflection through the junction. Note however that wave signals

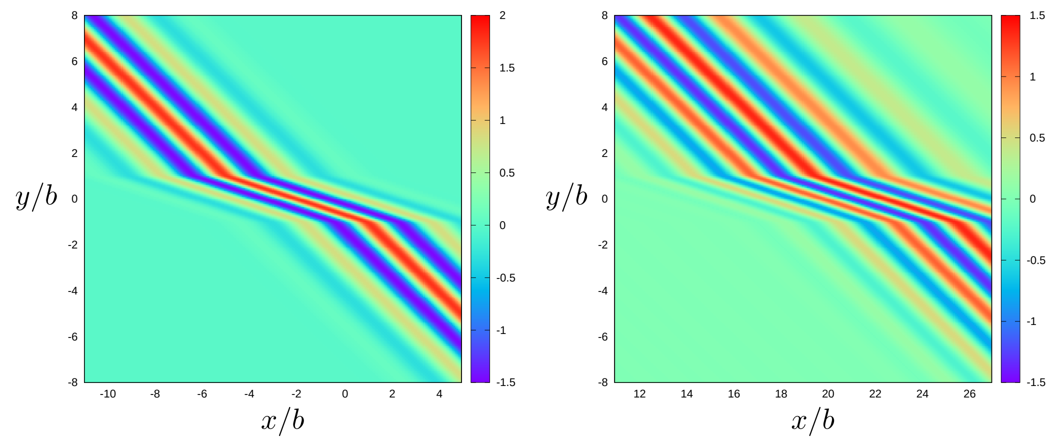

Figure 4: The instantaneous surface wave amplitude for a $\theta_0 = 45^\circ$ directed Gaussian wave packet defined in (a) at $t = 0$ and evolving to (b) at $t = 6$s for an array of plates tilted at $\delta = -45^\circ$ in water of constant depth.

will not be perfectly reconstructed beyond the junction since the phase shift in the transmission coefficient is frequency dependent.

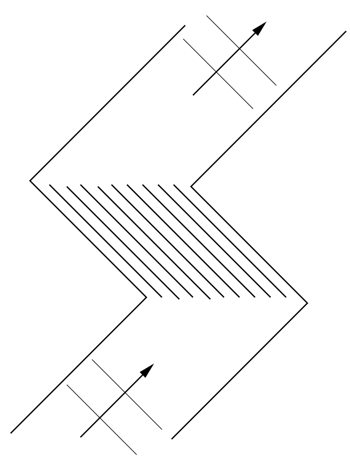

Figure 5: A schematic of an all-wavenumber perfectly-transmitting waveguide junction.

3.3. Gaussian beam

The result listed (ii)(b) in §3.1 is the well-known resonance effect due coherent interference of waves propagating between the two ends of the narrow channels in the array. In contrast to the first listed result (ii)(a) this phenomenon is independent of incident wave direction, θ_0, and array inclination, δ. Thus the titled plate array can act as an all-angle perfectly-transmitting negative-refraction metamaterial waveshifter at specific frequencies. It also provides us with better way of visualising the negative refraction property of the plate array by illuminating it with a Gaussian beam. A Gaussian beam field can be constructed by weighting plane wave solutions over a range of incident wave angles (see, for e.g. [11, §3]) according to

$$\phi_b(x,y) = \sqrt{4\pi}\int_{\theta_b-\Delta\theta_b}^{\theta_b+\Delta\theta_b} \cos(\theta_b-\theta_0)\mathrm{e}^{-4\pi^2\sin^2(\theta_b-\theta_0)}\phi(x,y;\theta_0)\,d\theta_0 \tag{3.26}$$

where $\phi(x,y;\theta_0)$ refers to the plane wave solution of §3.1 under an incident angle θ_0. The principal direction of the beam is given by θ_b and $\Delta\theta_b$ provides a numerical cut-off to the Gaussian envelope chosen, for simplicity, so that only real scattering angles are selected in the integration. Again, this is computed using the rectangle rule. A snapshot of the wave amplitude of the time-harmonic solution provided by $\Re\{\phi_b(x,y)\}$ is shown in Fig. 6 for $\theta_b = 45°$ and $\delta = -45°$ and the wavenumber $kL = 9\pi/2$ satisfies the criterion for total transmission.

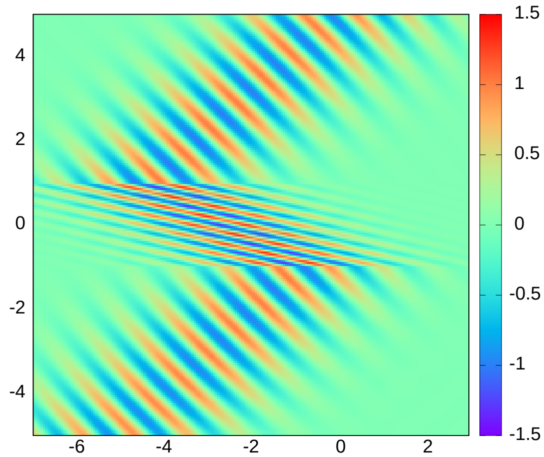

Figure 6: Perfect transmission of a Gaussian beam incidence at 45° on a staggered array $\delta = -45°$ at $kL = 9\pi/2$.

3.4. Edge waves

In this section we consider the existence of localised wave modes capable of propagating along the plate array whilst decaying away from the array. Such waves are commonly referred to as trapped waves, guided waves or edge waves depending upon the physical context. Although they cannot be excited by plane incident waves considered in §3.1 the importance of such solutions is highlighted in the next section where we will show that they are excited by a wave source in the vicinity of the effective medium; a related problem in electromagnetic theory can be found in [12].

The solution in $|y| < b$ is still described by (3.10) but instead of incident, reflected and transmitted waves in $|y| > b$ the general solution in $y < -b$ is replaced by

$$\phi_e(x,y) = A\mathrm{e}^{\pm\mathrm{i}\alpha_e x}\mathrm{e}^{\gamma_e(y+b)} \tag{3.27}$$

and in $y > b$,

$$\phi_e(x,y) = B\mathrm{e}^{\pm\mathrm{i}\alpha_e x}\mathrm{e}^{-\gamma_e(y-b)} \tag{3.28}$$

where A and B are to be determined and $\alpha_e > k$ while $\gamma_e = \sqrt{\alpha_e^2 - k^2}$. In the scattering problem of §3.1 $\alpha_0 = k \sin\theta_0 < k$ in modulus was used in place of α_e and the choice $\alpha_e > k$ forces the wave field to decay away from the array. This alone is insufficient to establish the existence of localised waves as these general expressions need to be matched to the general expression for the wave field in $|y| < b$.

There is no difference to the matching procedure used in §3.1 and matching $\phi(x, -b)$ from inside and outside the plate array using (3.10) and (3.27) gives

$$C'\mathrm{e}^{\pm \mathrm{i}\alpha_e b \tan\delta}\mathrm{e}^{-\mathrm{i}kb/\cos\delta} + D'\mathrm{e}^{\pm \mathrm{i}\alpha_e b \tan\delta}\mathrm{e}^{\mathrm{i}kb/\cos\delta} = A \tag{3.29}$$

where C' and D' are related to the functions C and D via (3.11) with $\pm\alpha_e$ replacing α_0. This simplifies to

$$C'\mathrm{e}^{-\mathrm{i}kb/\cos\delta} + D'\mathrm{e}^{\mathrm{i}kb/\cos\delta} = A' \tag{3.30}$$

after use of the abbreviation $A = A'\mathrm{e}^{\pm \mathrm{i}\alpha_e b \tan\delta}$. Matching fluxes across $y = -b$ provides a second relation between the coefficients C', D' and A' of

$$\mathrm{i}k\cos\delta(C'\mathrm{e}^{-\mathrm{i}kb/\cos\delta} - D'\mathrm{e}^{\mathrm{i}kb/\cos\delta}) = \gamma_e A'. \tag{3.31}$$

Following the same process of matching ϕ and the fluxes across $y = b$ readily gives two further relations, namely

$$C'\mathrm{e}^{\mathrm{i}kb/\cos\delta} + D'\mathrm{e}^{-\mathrm{i}kb/\cos\delta} = B' \tag{3.32}$$

where $B = B'\mathrm{e}^{\mp c i \alpha_e b \tan\delta}$ and

$$\mathrm{i}k\cos\delta(C'\mathrm{e}^{\mathrm{i}kb/\cos\delta} - D'\mathrm{e}^{-\mathrm{i}kb/\cos\delta}) = -\gamma_e B'. \tag{3.33}$$

Using $L = b/\cos\delta$ and eliminating A' and B' from (3.30), (3.31) and (3.32), (3.32) results in the system

$$\begin{pmatrix} (\gamma_e - \mathrm{i}k\cos\delta)\mathrm{e}^{-\mathrm{i}kL} & (\gamma_e + \mathrm{i}k\cos\delta)\mathrm{e}^{\mathrm{i}kL} \\ (\gamma_e + \mathrm{i}k\cos\delta)\mathrm{e}^{\mathrm{i}kL} & (\gamma_e - \mathrm{i}k\cos\delta)\mathrm{e}^{-\mathrm{i}kL} \end{pmatrix} \begin{pmatrix} C' \\ D' \end{pmatrix} = 0 \tag{3.34}$$

and it follows that non-trivial solutions correspond to the vanishing of the determinant which can be written as the condition

$$(\gamma_e^2 - k^2\cos^2\delta)\sin(2kL) + 2\gamma_e k\cos\delta\cos(2kL) = 0. \tag{3.35}$$

This equation is quadratic in γ_e and solutions given by either $\gamma_e = k\cos\delta\tan(kL)$ or $\gamma_e = -k\cos\delta\cot(kL)$. Since $\cos\delta > 0$ and we require $\gamma_e > 0$ for decay at infinity, values of kL such that $\tan(kL)$ is positive give edge waves defined by

$$\alpha_e = k(1 + \cos^2\delta\tan^2(kL))^{1/2} \tag{3.36}$$

and in complementary intervals $-\cot(kL)$ is positive whence

$$\alpha_e = k(1 + \cos^2\delta\cot^2(kL))^{1/2}. \tag{3.37}$$

We finish this section with a discussion of the special case $\delta = 0$ since the edge wave solutions derived here can be compared to the results of [13]. They considered the problem of edge waves along a periodic array of thin plates without stagger but made no assumption on the spacing between neighbouring plates. Their expression (eqn. (2.49) in [13]) for edge waves having a plane of symmetry along $y = 0$ expressed in the current notation is

$$\begin{aligned} kL \,=\, & (n + \tfrac{1}{2})\pi + (kd/\pi)\ln 2 - \sin^{-1}(k/\alpha_e) \\ & - \sum_{m=1}^{\infty}\left[\sin^{-1}\left(\frac{k}{\alpha_e + 2m\pi/d}\right) + \sin^{-1}\left(\frac{k}{\alpha_e + 2m\pi/d}\right) - \sin^{-1}\left(\frac{kd}{m\pi}\right)\right] \end{aligned} \tag{3.38}$$

($n \in \mathbb{Z}$) and was derived using a powerful Modified Residue Calculus method. In the limit $d/L \to 0$ with $kL = O(1)$ (3.38) reduces to

$$\alpha_e = k(-1)^n/\cos(kL) \tag{3.39}$$

coinciding with our condition (3.36) for $\delta = 0$. The ambiguity in the sign of α_e is reflected in the opening assumption (3.27). These represent guided modes which are symmetric about $y = 0$. For modes antisymmetric about $y = 0$, the result of [13] only requires $(n + \frac{1}{2})\pi$ to be replaced by $n\pi$ in (3.38) and it follows that (3.39) is replaced by $\alpha_e = k(-1)^n/\sin(kL)$ which coincides with our condition (3.37) when $\delta = 0$.

3.5. Diffraction from a source

We can use the description of the plate array under effective medium theory developed in §3.1 to solve more general wave diffraction problems. The canonical problem is radiation from a wave source placed outside the plate array. We replace the incident plane wave field of §3.1 by a a two-dimensional outgoing wave source at $(x, y) = (0, -c)$ where $c > b$ which is given by

$$\phi_{inc}(x, y) = H_0^{(1)}(k\sqrt{x^2 + (y + c)^2}) = \frac{1}{\pi}\int_{-\infty}^{\infty} \frac{\mathrm{e}^{\mathrm{i}\alpha x}\mathrm{e}^{\mathrm{i}\beta|y+c|}}{\beta}d\alpha, \tag{3.40}$$

using the standard Fourier transform representation of the Hankel function $H_0^{(1)}$. In the above $\beta = \sqrt{k^2 - \alpha^2} = \mathrm{i}\gamma \equiv \mathrm{i}\sqrt{\alpha^2 - k^2}$, the former appropriate for $|\alpha| \leq k$, the latter for $|\alpha| \geq k$. For $y > -c$, (3.41) is

$$\phi_{inc}(x, y) = \frac{1}{\pi}\int_{-\infty}^{\infty} \frac{\mathrm{e}^{\mathrm{i}\beta c}}{\beta}\mathrm{e}^{\mathrm{i}\alpha x}\mathrm{e}^{\mathrm{i}\beta y}d\alpha \tag{3.41}$$

which is a weighted integral over plane incident waves with wavenumber components α and β in the x and y directions. Thus, we can infer the total field in $y < -b$ to be the sum of the source and same weighted integral over plane waves reflected from the effective medium occupying $|y| < b$ and written as

$$\phi_s(x,y) = \phi_{inc}(x,y) + \frac{1}{\pi}\int_{-\infty}^{\infty} \frac{\mathrm{e}^{\mathrm{i}\beta c}}{\beta} R(\sin^{-1}(\alpha/k), \delta, kL)\mathrm{e}^{\mathrm{i}\alpha x}\mathrm{e}^{-\mathrm{i}\beta y} d\alpha \tag{3.42}$$

whilst in $y > b$ the field is written

$$\phi_s(x,y) = \frac{1}{\pi}\int_{-\infty}^{\infty} \frac{\mathrm{e}^{\mathrm{i}\beta c}}{\beta} T(\sin^{-1}(\alpha/k), \delta, kL)\mathrm{e}^{\mathrm{i}\alpha x}\mathrm{e}^{\mathrm{i}\beta y} d\alpha \tag{3.43}$$

where R and T represent the reflection and transmission coefficients defined in (3.17) and (3.18). Note that, in the notation of §3, α represents the value $k \sin\theta_0$ and so $\cos\theta_0$ thus equates to β/k. This equality extends to non-real scattering angles (that is when $|\alpha| > k$) when $\cos\theta_0$ equates to $\mathrm{i}\gamma/k$.

For example, in $y < -b$ (3.42) explicitly reads

$$\phi_s(x,y) = \phi_{inc}(x,y) + \frac{1}{\pi}\int_{-\infty}^{\infty} \frac{\mathrm{e}^{\mathrm{i}\beta c}}{\beta} \frac{(\beta^2 - k^2\cos^2\delta)\sin(2kL)\mathrm{e}^{-2\mathrm{i}\beta L\cos\delta}}{(\beta^2 + k^2\cos^2\delta)\sin(2kL) + 2\mathrm{i}\beta k\cos(2kL)\cos\delta}\mathrm{e}^{\mathrm{i}\alpha x}\mathrm{e}^{-\mathrm{i}\beta y}\, d\alpha. \tag{3.44}$$

Careful consideration of the integrand for values of $|\alpha| > k$, when we replace $\beta = \mathrm{i}\gamma$ (γ real), reveals that there are poles in the integrand for real values of $\alpha = \pm\alpha_e$ satisfying (3.36) or (3.37) where $\gamma = \gamma_e = k\cos\delta\tan(kL)$ or $-k\cos\delta\cot(kL)$ (respectively) and (3.35) is satisfied. Therefore the integral in (3.44) originating from the inverse Fourier integral in the definition (3.40) must be deformed from the real α-axis to avoid these poles. Physically, the energy from a wave source crossing a straight boundary consists of an appropriately-weighted spectrum of plane waves over all real and non-real scattering angles and some this energy may feed into the edge waves predicted by §3.4 and supported by the effective medium.

The sense in which the deformation around the poles is made must ensure those edge waves propagate energy away from the source. The definitions of (3.36) or (3.37) ensure that $d\alpha_e/dk > 0$ and this implies the contour should be deformed under/over at $\alpha = \pm\alpha_e$ respectively. We can shrink this deformation onto the real α-axis, thereby evaluating the contribution from vanishly-small semi-circular indentations around the poles to give

$$\begin{aligned}\phi_s(x,y) \quad = \quad & \phi_{inc}(x,y) + \frac{2}{\pi}\int_0^{\pi/2} \frac{(\cos^2\theta - \cos^2\delta)\sin(2kL)\mathrm{e}^{\mathrm{i}k(c-y-2b)\cos\theta}\cos(kx\sin\theta)}{(\cos^2\theta + \cos^2\delta)\sin(2kL) + 2\mathrm{i}\cos\theta\cos\delta\cos(2kL)}\, d\theta \\ & -\frac{2\mathrm{i}}{\pi}\int_0^{\infty} \frac{(\sinh^2 v + \cos^2\delta)\sin(2kL)\mathrm{e}^{-k(c-y-2b)\sinh v}\cos(kx\cosh v)}{(\sinh^2 v - \cos^2\delta)\sin(2kL) + 2\sinh v\cos\delta\cos(2kL)}\, dv \\ & + \tanh v_e \mathrm{e}^{-k(c-y-2b)\sinh v_e}\mathrm{e}^{\mathrm{i}k|x|\cosh v_e)}\end{aligned} \tag{3.45}$$

where the semi-infinite integral is of Cauchy principal-value type and $\alpha_e = \cosh v_e$, $\gamma_e = \sinh v_e$ is as a result of a change of integration variable.

An analogous decomposition of the field in $y > b$ can be made to find that (3.43) can be expressed as

$$\begin{aligned}\phi_s(x,y) &= \frac{4\mathrm{i}}{\pi}\int_0^{\pi/2}\frac{\cos\theta\ \cos\delta\,\mathrm{e}^{\mathrm{i}k(c+y-2b)\cos\theta}\cos\{k(x-2b\tan\delta)\sin\theta\}}{(\cos^2\theta+\cos^2\delta)\sin(2kL)+2\mathrm{i}\cos\theta\cos\delta\cos(2kL)}\,d\theta\\ &\quad-\frac{4\mathrm{i}}{\pi}\int_0^{\infty}\frac{\sinh v\ \cos\delta\,\mathrm{e}^{-k(c+y-2b)\sinh v}\cos\{k(x-2b\tan\delta)\cosh v\}}{(\sinh^2 v-\cos^2\delta)\sin(2kL)+2\sinh v\cos\delta\cos(2kL)}\,dv\\ &\quad+\tanh v_e \mathrm{e}^{-k(c+y-2b)\sinh v_e}\mathrm{e}^{\mathrm{i}k|x-2b\tan\delta|\cosh v_e}. \end{aligned} \tag{3.46}$$

The field within the plate array can be similarly represented using the information in §3.1 to define $\phi(x,y)$ in $|y| < b$. For completeness, we provide the result of this algebraically complex calculation here as

$$\begin{aligned}\phi_s(x,y) &= \frac{2\mathrm{i}}{\pi}\int_0^{\pi/2}\frac{\cos\theta\,\mathrm{e}^{\mathrm{i}k(c-b)\cos\theta}\cos\{k(x-(y+b)\tan\delta)\sin\theta\}}{(\cos^2\theta+\cos^2\delta)\sin(2kL)+2\mathrm{i}\cos\theta\cos\delta\cos(2kL)}M(\theta,y)\,d\theta\\ &\quad-\frac{2\mathrm{i}}{\pi}\int_0^{\infty}\frac{\sinh v\ \cos\delta\,\mathrm{e}^{-k(c-b)\sinh v}\cos\{k(x-(y+b)\tan\delta)\cosh v\}}{(\sinh^2 v-\cos^2\delta)\sin(2kL)+2\sinh v\cos\delta\cos(2kL)}N(v,y)\,dv\\ &\quad+\tfrac{1}{2}\tanh v_e \mathrm{e}^{-k(c-b)\sinh v_e}\mathrm{e}^{\mathrm{i}k|x-(y+b)\tan\delta|\cosh v_e}N(v_e,y). \end{aligned} \tag{3.47}$$

for $|y| < b$, where

$$M(\theta,y) = (1+\cos\theta/\cos\delta)\mathrm{e}^{-\mathrm{i}k(b-y)/\cos\delta} + (1-\cos\theta/\cos\delta)\mathrm{e}^{\mathrm{i}k(b-y)/\cos\delta}$$

and

$$N(v,y) = (1+\mathrm{i}\sinh v/\cos\delta)\mathrm{e}^{-\mathrm{i}k(b-y)/\cos\delta} + (1-\mathrm{i}\sinh v/\cos\delta)\mathrm{e}^{\mathrm{i}k(b-y)/\cos\delta}.$$

As in the Gaussian beam problem of §3.4, when a point source is excited at a frequency which coincides with all-angle perfect transmission of the plate array (i.e. $\sin(2kL) = 0$) the only effect of the array will be to shift the position of the source on the far side of the array by the amount $2b\tan\delta$. For example in (3.45) the solution when $\sin(2kL) = 0$ in $y < -b$ is just ϕ_{inc}, the source, with no reflection from the plate array. An example of perfect transmission is illustrated in Fig. 7(a) where $kL = 4\pi$ is used for a $\delta = 60°$ plate array. In contrast, Fig. 7(b) uses $kL = 5/\cos(\pi/6) \approx 5.77$ a value of no special significance for a $\delta = 30°$ array and now there is partial reflection and transmission by the array whilst some of energy from the source is transported to infinity along the array itself in the form of edge waves which appear as the repeating oscillations confined to the plate array.

4. Exact treatment of the scattering problem

In this section we set about solving the problem of plane wave scattering by a periodic array of titled plates without making a close-spacing approximation.

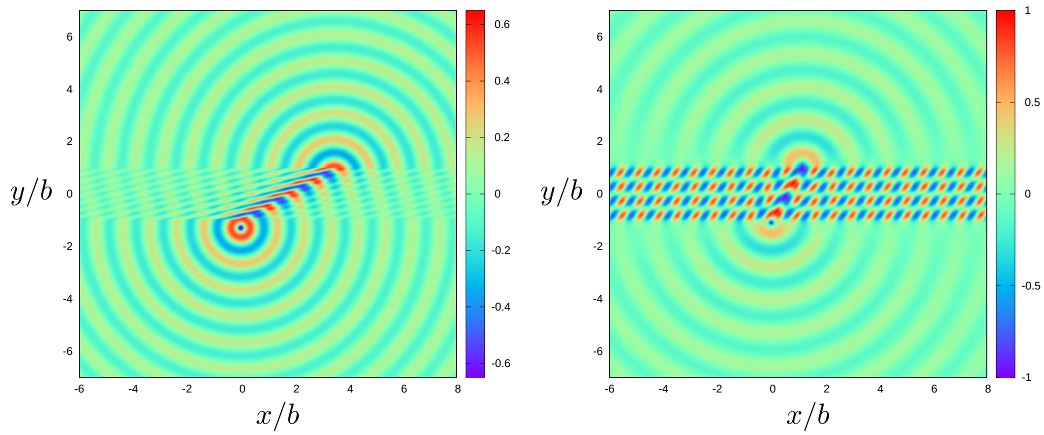

Figure 7: The instantaneous surface wave amplitudes for: (a) a $\delta = 60^\circ$ plate array with a wave source at $c/b = 1.3$ with $kL = 4\pi$; and (b) $\delta = 30^\circ$, $c/b = 1.1$ with $kL = 5.77$.

On account of the periodicity of the geometry and the form of the incident wave it must be that

$$\phi(x+l, y) = \mathrm{e}^{\mathrm{i}\alpha_0 l}\phi(x, y). \tag{4.1}$$

The idea is to exploit the periodicity and to solve the problem in a single fundamental strip, aligned with the array, allowing the solution outside this strip to be determined by (4.1). Thus, we are required to consider the problem in rotated (X, Y) coordinates as defined by (2.4).

First, from (2.2) we write $\phi_{inc}(x, y) \equiv \psi_{inc}(X, Y) = \mathrm{e}^{\mathrm{i}A_0^+ X}\mathrm{e}^{\mathrm{i}B_0^+ Y}$ where $A_0^\pm = k\sin(\theta_0 \mp \delta)$ and $B_0^\pm = k\cos(\theta_0 \mp \delta)$. Likewise, $\phi(x, y) \equiv \psi(X, Y)$, and periodicity, (4.1), under the transformed coordinates implies

$$\psi(X+d, Y+a) = \mathrm{e}^{\mathrm{i}\alpha_0 l}\psi(X, Y) \equiv \mathrm{e}^{\mathrm{i}A_0^+ d}\mathrm{e}^{\mathrm{i}B_0^+ a}\psi(X, Y) \tag{4.2}$$

where we note that $\alpha_0 l = A_0^+ d + B_0^+ a = A_0^- d - B_0^- a$. Far away from the grating the conditions (2.3) are transformed into

$$\psi(X, Y) \sim \begin{cases} \mathrm{e}^{\mathrm{i}A_0^+ X}\mathrm{e}^{\mathrm{i}B_0^+ Y} + R\mathrm{e}^{\mathrm{i}A_0^- X}\mathrm{e}^{-\mathrm{i}B_0^- Y}, & \text{as } Y \to -\infty, \\ T\mathrm{e}^{\mathrm{i}A_0^+ X}\mathrm{e}^{\mathrm{i}B_0^+ Y}, & \text{as } Y \to \infty. \end{cases} \tag{4.3}$$

The periodicity allows us to restrict attention to a single strip $0 < X < d$ and $-\infty < Y < \infty$. It follows that within this strip

$$\psi_X(0^+, Y) - \mathrm{e}^{-\mathrm{i}\alpha_0 l}\psi_X(d^-, Y+a) = 0 \tag{4.4}$$

for all Y since $\psi_X = 0$ on both sides of the plates. Additionally we have

$$\psi(0^+, Y) - \mathrm{e}^{-\mathrm{i}\alpha_0 l}\psi(d^-, Y+a) = \begin{cases} p(Y), & |Y| < L, \\ 0, & |Y| > L \end{cases} \tag{4.5}$$

since ψ is continous across the boundaries $X = 0$ and $X = d$ when $|Y| > L$ but not otherwise. In (4.5) $p(Y)$ represents the jump in ψ across the plate centred at the origin.

We define Fourier transforms in Y, writing

$$\Psi(X, \beta) = \int_{-\infty}^{\infty} (\psi(X, Y) - \psi_{inc}(X, Y))\mathrm{e}^{-\mathrm{i}\beta Y} dY. \tag{4.6}$$

Taking transforms of the wave equation gives solutions in $0 < X < d$ of

$$\Psi(X, \beta) = C(\beta) \cosh \gamma X + D(\beta) \cosh \gamma(X - d) \tag{4.7}$$

where $\gamma = \sqrt{\beta^2 - k^2} = -\mathrm{i}\sqrt{k^2 - \beta^2}$. This general solution must satisfy the two transformed conditions (4.4) and (4.5) namely

$$\Psi_X(0, \beta) - \mathrm{e}^{-\mathrm{i}\alpha_0 l}\mathrm{e}^{\mathrm{i}\beta a}\Psi_X(d, \beta) = 0 \tag{4.8}$$

and

$$\Psi(0, \beta) - \mathrm{e}^{-\mathrm{i}\alpha_0 l}\mathrm{e}^{\mathrm{i}\beta a}\Psi(d, \beta) = P(\beta) \tag{4.9}$$

where

$$P(\beta) = \int_{-L}^{L} p(Y)\mathrm{e}^{-\mathrm{i}\beta Y} dY \tag{4.10}$$

acts as a proxy in for $p(Y)$ in what follows. Applying (4.8) and (4.9) to (4.7) to determine the Fourier coefficients C and D in terms of P results in

$$\Psi(X, \beta) = P(\beta) \frac{(\mathrm{e}^{\mathrm{i}(\alpha_0 l - \beta a)} \cosh \gamma X - \cosh \gamma(X - d))}{2(\cos(\alpha_0 l - \beta a) - \cosh \gamma d)} \tag{4.11}$$

and so, by the inverse transform,

$$\psi(X, Y) = \psi_{inc}(X, Y) + \int_{-\infty}^{\infty} \frac{P(\beta)(\mathrm{e}^{\mathrm{i}(\alpha_0 l - \beta a)} \cosh \gamma X - \cosh \gamma(X - d))\mathrm{e}^{\mathrm{i}\beta Y}}{4\pi(\cos(\alpha_0 l - \beta a) - \cosh \gamma d)} d\beta \tag{4.12}$$

which is a representation for the function $\psi(X, Y)$ everywhere in the strip $0 < X < d$ in terms of the unknown $p(Y)$.

There are poles in the integrand at real values of $\beta < k$ satisfying

$$\mathrm{i}\gamma = \sqrt{k^2 - \beta^2} = (\alpha_0 l - \beta a + n\pi)/d, \tag{4.13}$$

where n is an integer and the inverse contour in (4.12) must be defined appropriately to avoid these poles.

Provided kd is small enough (as is assumed the case here), the only solutions (4.13) occur when $n = 0$ and when $\beta = \pm B_0^\pm$ with corresponding values of $\gamma = -\mathrm{i}A_0^\pm$. That is, there are two poles on the line of integration in the inverse transform representation of the solution in (4.12) at $\beta = \pm B_0^\pm$

and the contour of integration is chosen to pass above the pole at $\beta = -B_0^-$ and below the pole at $\beta = B_0^+$. This choice is made to fulfil the radiation conditions as $Y \to \pm\infty$ as stated in (4.3). Note that both $-B_0^-$ and B_0^+ can be either positive or negative depending on θ_0 and δ although $-B_0^- < B_0^+$.

Thus, as $Y \to \pm\infty$ we can deform the contour into the upper (lower) half β-plane and pick up the residue at $\beta = \pm B_0^\pm$ to give

$$\psi(X,Y) \sim \psi_{inc}(X,Y) + \frac{A_0^\pm P(\pm B_0^\pm)}{2kl\cos\theta_0}\mathrm{e}^{\mathrm{i}A_0^\pm X}\mathrm{e}^{\pm \mathrm{i}B_0^\pm Y} \tag{4.14}$$

as $Y \to \pm\infty$ and so it follows, by comparison with (4.3), that

$$T = 1 + \frac{A_0^+ P(B_0^+)}{2kl\cos\theta_0}, \qquad R = \frac{A_0^- P(-B_0^-)}{2kl\cos\theta_0}. \tag{4.15}$$

To determine the function $p(Y)$ we impose on (4.12) the condition $\partial_X\psi(0^+,Y) = 0$ for $|Y| < L$ to obtain the integral equation

$$4\pi\mathrm{i}A_0^+\mathrm{e}^{\mathrm{i}B_0^+Y} = \int_{-\infty}^{\infty}(E(\beta)+|\beta|)\mathrm{e}^{\mathrm{i}\beta Y}\int_{-L}^{L}p(Y')\mathrm{e}^{-\mathrm{i}\beta Y'}\,dY'\,d\beta, \qquad |Y| < L \tag{4.16}$$

in which

$$E(\beta) = \frac{\gamma\sinh\gamma d}{\cosh\gamma d - \cos(\alpha_0 l - \beta a)} - |\beta| \tag{4.17}$$

and $E(\beta) \sim -\frac{1}{2}k^2/|\beta|$ as $|\beta| \to \pm\infty$.

4.1. Numerical solution

In order to solve (4.16) numerically we first expand the unknown $p(Y)$ in a truncated finite series as follows:

$$p(Y) \approx 4\pi\mathrm{i}A_0^+L\sum_{n=0}^{N}a_n w_n(Y/L), \qquad |Y| < L \tag{4.18}$$

where

$$w_n(t) = \frac{\mathrm{e}^{\mathrm{i}\pi n/2}}{(n+1)}\sqrt{1-t^2}U_n(t) \tag{4.19}$$

and $U_n(\cos\theta) = \sin(n+1)\theta/\sin\theta$ is a second-kind Chebychev polynomial. This choice explicitly accounts for the anticipated square-root behaviour in the function $p(Y)$ as $|Y| \to L$ and provides the maximum simplification in the expressions that result. In particular we note the following results

$$W_n(\xi) = \int_{-1}^{1} w_n(t)\mathrm{e}^{-\mathrm{i}\xi t}dt = \begin{cases} J_{n+1}(\xi)/\xi, & \xi \neq 0 \\ \frac{1}{2}\delta_{n0}, & \xi = 0 \end{cases} \tag{4.20}$$

and

$$\int_{-\infty}^{\infty}\frac{J_{n+1}(\xi)J_{m+1}(\xi)}{|\xi|}d\xi = \frac{\delta_{mn}}{n+1} \tag{4.21}$$

([15, §6.538(2)])

Substituting (4.18) into (4.16), multiplying through by $w^*_m(Y/L)$ for $m = 0, \dots, N$ and integrating over $-L < Y < L$ results in the linear system of equations

$$\frac{a_m}{m+1} + \sum_{n=0}^{N} a_n K_{mn} = W_m(B_0^+ L) \tag{4.22}$$

where

$$K_{mn} = \int_{-\infty}^{\infty} \frac{LE(t/L)}{t^2} J_{n+1}(t) J_{m+1}(t) dt. \tag{4.23}$$

The integrals defining K_{mn} decay like $O(1/t^4)$ as $|t| \to \infty$ and are approximated by truncating at $t = \pm 100$. They must be calculated by evaluating the contributions from the poles at $t = \pm\beta_0^{\pm} L$ and leaving principal-value integrals behind. Specifically, this gives

$$K_{mn} \;=\; ⨍_{-\infty}^{\infty} \frac{LE(t/L)}{t^2} J_{n+1}(t) J_{m+1}(t) dt \tag{4.24}$$

$$-\frac{\pi \mathrm{i}}{kl\cos\theta_0}\{{A_0^+}^2 W_n(B_0^+ L) W_m(B_0^+ L) + {A_0^-}^2 W_n(-B_0^- L) W_m(-B_0^- L)\}. \tag{4.25}$$

Once solutions of (4.22) are calculated, R and T can be approximated by using (4.18) in (4.15) which leads to

$$T \approx 1 + \frac{2\pi \mathrm{i} k L^2 \sin^2(\theta_0 - \delta)}{l\cos\theta_0} \sum_{m=0}^{N} a_m W_m(B_0^+ L) \tag{4.26}$$

and

$$R \approx \frac{2\pi \mathrm{i} k L^2 \sin(\theta_0 - \delta)\sin(\theta_0 + \delta_0)}{l\cos\theta_0} \sum_{m=0}^{N} a_m W_m(-B_0^- L) \tag{4.27}$$

after use of the definition of $A_0^{\pm}$.

It is evident that $R = 0$ and $T = 1$ when $\theta_0 = \delta$, as required. Also clear is $R = 0$ when $\theta_0 = -\delta$. What is not evident from the results derived above is how solutions for an incident angle $-\theta_0$ are related to those for θ_0.

4.2. A scattering matrix formulation

In order to address the various properties that R and T possess, but which are not evident in the form expressed in (4.26), (4.27), it helps to adopt a more general but also slightly more complicated approach to solving the problem in which waves are allowed to be incident, with arbitrary amplitudes $A^{\pm}$ (say) from $y = \pm\infty$ respectively and give rise to outgoing waves of amplitudes $B^{\pm}$ as $y \to \mp\infty$. The same general methodology can be applied in this case and leads to the development of a scattering matrix, S which connects the incoming and outgoing wave amplitudes by

$$\begin{pmatrix} B^- \\ B^+ \end{pmatrix} = \mathsf{S} \begin{pmatrix} A^- \\ A^+ \end{pmatrix} \tag{4.28}$$

where

$$\mathsf{S} = \begin{pmatrix} T^- & R^+ \\ R^- & T^+ \end{pmatrix} \tag{4.29}$$

in which $R^\pm$, $T^\pm$ denote reflected and transmitted wave amplitudes due to incident waves from $y = \pm\infty$ respectively. In the previous sections R and T have been used for an incoming wave from $y = -\infty$ and so $R^- \equiv R$ and $T^- \equiv T$. The details of how this more general approach applies to the solution are ommitted (but see [14] to see the method applied to a similar problem) and it can be shown that

$$\mathsf{S} = (\mathsf{I} - \mathrm{i}\mu\mathsf{APA})^{-1}(\mathsf{I} + \mathrm{i}\mu\mathsf{APA}) \tag{4.30}$$

where $\mu = \pi/(kl\cos\theta_0)$, I is the 2×2 identity matrix,

$$\mathsf{A} = \begin{pmatrix} A_0^+ & 0 \\ 0 & A_0^- \end{pmatrix} \qquad \text{and} \qquad \mathsf{P} = \begin{pmatrix} P^+(B_0^+) & P^-(B_0^+) \\ P^+(-B_0^-) & P^-(-B_0^-) \end{pmatrix}. \tag{4.31}$$

Here, $P^\pm(\beta)$ satisfy

$$\fint_{-\infty}^{\infty} P^\pm(\beta)\mathrm{e}^{\mathrm{i}\beta Y}(E(\beta) + |\beta|)d\beta = \mathrm{e}^{\pm\mathrm{i}B_0^\pm Y}, \qquad |Y| < L \tag{4.32}$$

which is a modified version of (4.15) in which the integral is of Cauchy principal-value type.

Useful properties of the solution can be inferred from these two integral equations. First, by taking the complex conjugate of (4.32) and then replacing Y by $-Y$ we find that the complex conjugate $\overline{P^\pm(\beta)}$ satisfy the same equation as $P^\pm(\beta)$ and hence $P^\pm(\beta)$ are real.

Next, if we multiply (4.32) respectively by the two surrogate functions $\overline{p^\pm(Y)}$ and integrate over $|Y| < L$ we find that

$$P^-(B_0^+) = \fint_{-\infty}^{\infty} P^+(\beta)P^-(\beta)(E(\beta) + |\beta|)d\beta = P^+(-B_0^-) \tag{4.33}$$

after using the realness of $P^\pm$.

Also, we may take complex conjugates of (4.32), make the substitution $\beta \to -\beta$ in the integral and simultaneously switch $\delta \to -\delta$ (using relations $E(-\beta; -\delta) = E(\beta; \delta)$ and $B_0^\pm(-\delta) = B_0^\mp(\delta)$) to get

$$\fint_{-\infty}^{\infty} P^\pm(-\beta)\mathrm{e}^{\mathrm{i}\beta Y}(E(\beta) + |\beta|)d\beta = \mathrm{e}^{\mp\mathrm{i}B_0^\mp Y}, \qquad |Y| < L \tag{4.34}$$

and it therefore follows that $P^\pm(-\beta) = P^\mp(\beta)$. Thus, we infer that only one solution $P^+(\beta)$, say, is required and the other follows from it. In particular, we conclude that

$$\mathsf{P} = \begin{pmatrix} P^+(B_0^+) & P^+(-B_0^+) \\ P^+(-B_0^-) & P^+(B_0^-) \end{pmatrix}, \tag{4.35}$$

expressed entirely in terms of P^+ and is real and symmetric. It follows from (4.30) that $\mathsf{S}\overline{\mathsf{S}} = \mathsf{I}$ which can be used to prove various identities satisfied by $R^\pm$ and $T^\pm$. However, as these do not include conservation of energy it turns out to be a distraction. Thus it is more straightforward to make a direct computation of the reflection and transmission coefficients from (4.30) as

$$R^+ = R^- = \frac{2\mathrm{i}\mu A_0^+ A_0^- \mathsf{P}_{12}}{(1 - \mathrm{i}\mu {A_0^+}^2 \mathsf{P}_{11})(1 - \mathrm{i}\mu {A_0^-}^2 \mathsf{P}_{22}) + \mu^2 {A_0^-}^2 {A_0^+}^2 \mathsf{P}_{12}^2} \tag{4.36}$$

and

$$T^\pm = \frac{(1 \mp \mathrm{i}\mu {A_0^+}^2 \mathsf{P}_{11})(1 \pm \mathrm{i}\mu {A_0^-}^2 \mathsf{P}_{22}) - \mu^2 {A_0^-}^2 {A_0^+}^2 \mathsf{P}_{12}^2}{(1 - \mathrm{i}\mu {A_0^+}^2 \mathsf{P}_{11})(1 - \mathrm{i}\mu {A_0^-}^2 \mathsf{P}_{22}) + \mu^2 {A_0^-}^2 {A_0^+}^2 \mathsf{P}_{12}^2} \tag{4.37}$$

implying that $|T^-| = |T^+|$. With more work, not shown here, the conservation of energy relations can be shown to be satisfied exactly.

We can now readily confirm that $R^\pm = 0$ when $\theta_0 = \pm\delta$ and that $T^+ = 1$, $|T^-| = 1$ when $\theta = -\delta$ and that $T^- = 1$, $|T^+| = 1$ when $\theta_0 = \delta$.

We can also confirm the all properties relating to angles listed in §3.1. For example, letting $\delta \to -\delta$ is geometrically equivalent to reversing the direction of the incident wave so that values of R^+ and R^- and T^+ and T^- are interchanged. It follows that $R(\theta_0, \delta, kL) = R(\theta_0, -\delta, kL)$. Similarly, negating θ_0 and δ simultaneously does not alter the problem and so $R(-\theta_0, -\delta, kL) = R(\theta_0, \delta, kL) = R(-\theta_0, \delta, kL)$ by the preceding result and this proves symmetry with respect to θ_0. Finally, it is evident from (4.36) that $R(\theta_0, \delta, kL) = -R(\delta, \theta_0, kL)$.

The exact R and T do not share wavenumber periodicity, expressed by property (iv) in §3.1. In particular, extra channel modes and diffraction modes will eventually be cut on as the frequency increases.

Implementation of a numerical solution for this scattering matrix approach is virtually the same as in §4.1, but instead of (4.22) we only need to solve a real system of equations for real coefficients a_n as K_{mn} is replaced by $\Re\{K_{mn}\}$, then

$$\mathsf{P}_{11} \approx L \sum_{n=0}^{N} a_n W_m(B_0^+ L), \qquad \mathsf{P}_{12} \approx L \sum_{n=0}^{N} a_n W_m(-B_0^+ L), \tag{4.38}$$

and

$$\mathsf{P}_{22} \approx L \sum_{n=0}^{N} a_n W_m(B_0^- L). \tag{4.39}$$

define the real elements of P and $R^\pm$, $T^\pm$ are subsequently determined by (4.36), (4.37).

In Fig. 8 we compare the results of the exact problem with results from the approximation in §3.1. Although the exact results (dashed curves) in Fig. 8(a) appear to be periodic, they are not: only in the limit $d = 0$ (solid curve).

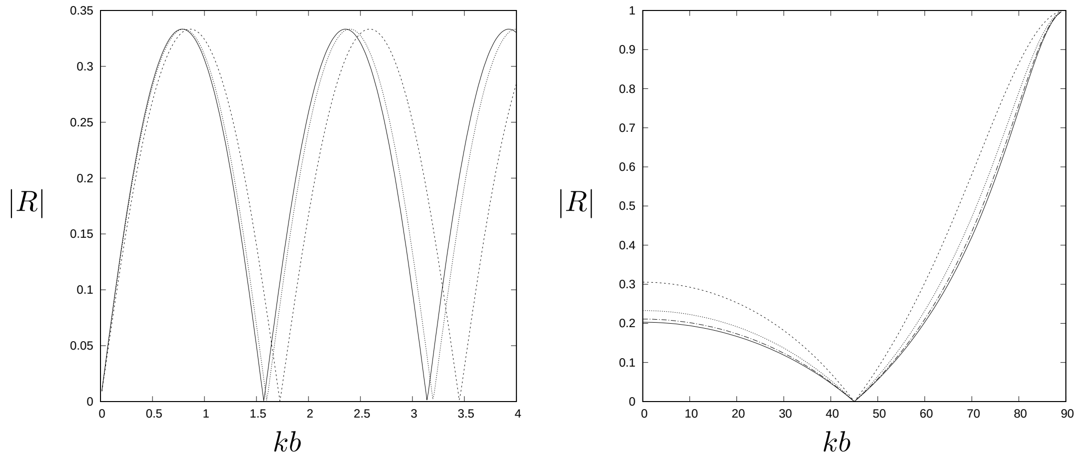

Figure 8: The convergence exact results for $|R|$ towards approximate results (solid curves) as the array spacing decreases. In the left-hand panel $|R|$ against kb for $\delta = 45^\circ$, $\theta_0 = 0$ and $d/L = 0.1, 0.01$ and solid curve computed using (3.16). In right-hand panel, exact $|R|$ as θ_0 varies for $\delta = 45^\circ$, $kb = 2$ and $d/L = 0.5, 0.1, 0.02$ (dashed curves) converging to the solid curve computed from (3.16).

5. Conclusion

Scattering of waves by an infinite periodic array of inclined (or staggered) thin parallel plates occupying a region of finite width and infinite length has been considered. An approximation has been developed based on close spacing between plates, relative to their length, within the array allowing region occupied by the plate array to be replaced by an effective medium and matching conditions on the boundary of the plate array replaced by effective matching conditions. This reduction in complexity leads to simple explicit expressions for wave scattering of plane incident waves, wave sources and for guided waves along the array.

Solutions to the exact geometrical description of the problem have been computed by formulating solutions using Bloch-Floquet theory and integral equations. These have been shown to converge to the close-spacing approximation when the separation between plates tends to zero, confirming that the approximation can be used with good accuracy for sufficiently small spacing to plate length ratios. Moreover they confirm that several key properties of the reflection and transmission coefficient are shared by the approximation and the exact treatment of the problem. This includes total transmission for all wavenumbers when the inclination of the plates within the array are opposed to the incident wave direction and for all wave angles and plate inclinations for certain specific frequencies. This allows us to use the finite width plate array as an perfectly-transmitting negative refraction material allowing perfect waveshifting across the plate array. For example, wave sources can be shifted to 'spoof' the location of a source through an array. Plate arrays can also be used to perfectly transmit wave energy of all frequencies through a junction in a waveguide.

The anisotropic scattering provided by plate arrays are being considered in other settings, using the effective medium theory developed here to simplify solutions. Recently they have been used by [16] as a broadbanded sound absorption device when embedded in a trapezoidal cavity attached to the walls of a waveguide. They have also been used by [17] to redirect and absorb energy in cylinders formed by plate arrays in a water wave setting.

References

[1] A.J. Cooper & N. Peake, Upstream-radiated rotor-stator interaction noise in mean swirling flow. *J. Fluid Mech.* **523** 219–250, 2005.

[2] S. Kaji & T. Okazaki, Propagation of sound waves through a blade row. *J. Sound Vib.* **11**(3), 339–355, 1970.

[3] R. Mani & G. Horvay, Sound transmission through blade rows. *J. Sound Vib.* **12**(1), 59–83, 1970.

[4] W. Koch, On the transmission of sound waves through a blade row. *J. Sound Vib.* **18**(1), 111–128, 1971.

[5] J.F. Carlson & A.E. Heins, The reflection of an electromagnetic plane wave by an infinite set of plates, II. *Quart. Appl. Math.* **4**, 313–329, 1947.

[6] A.E. Heins & J.F. Carlson, Reflection of an electromagnetic plane wave by an infinite set of plates, II. *Quart. Appl. Math.* **5**, 82–88, 1948.

[7] A.E. Heins, Reflection of an electromagnetic plane wave by an infinite set of plates, III. *Quart. Appl. Math.* **8**, 281–291, 1950.

[8] C.M. Park & S.H. Lee, Zero-reflection acoustic metamaterial with a negative refractive index. *Sci. Rep.* 9:3372, 2019.

[9] H. Chen & C.T. Chan, Electromagnetic wave manipulation by layered systems using the transformation media concept. *Phys. Rev. B* **78** 054204, 2008.

[10] C.P. Berraquero, A. Maurel, P. Petitjeans & V. Pagneux, Experimental realization of a water-wave metamaterial shifter. *Phys. Rev. E* **88** 051002, 2013.

[11] M.J.A. Smith, R.C. McPhedran, C.G. Poulton & M.H. Meylan, Negative refraction and dispersion phenomena in platonic clusters. *Waves in Random and Complex Media* **22**(4), 435–458, 2012.

[12] R.E. Collin, *Field Theory of Guided Waves* IEEE Press, p.725, 1991.

[13] D.V. Evans & C.M. Linton, Edge waves along periodic coastlines. *Quart. J. Mech. Appl. Math.* **46**(4), 643–656, 1993.

[14] R. Porter, Linearised water wave problems involving submerged horizontal plates. *Appl. Ocean. Res.* **50** 91–109, 2015.

[15] I.S. Gradshteyn & I.M. Ryzhik. Table of Integrals Series and Products. Academic Press, 1980.

[16] A.U. Jan & R. Porter, Transmission and absorption in a waveguide with a metamaterial cavity. *J. Acoust. Soc. Am.* **144**(6) 3172–3180, 2018.

[17] S. Zheng, R. Porter & D. Greaves, Wave scattering by an array of metamaterial cylinders. *Under consideration for publication in J. Fluid Mech.*, 2020.